Check for
updates

Optimizing precision irrigation of a vineyard to improve water use efficiency and profitability by using a decision-oriented vine water consumption model

J. Bellvert[1] · M. Mata[1] · X. Vallverdú[1] · C. Paris[1] · J. Marsal[1]

Abstract

While the agronomic and economic benefits of regulated deficit irrigation (RDI) strategies have long been established in red wine grape varieties, spatial variability in water requirements across a vineyard limits their practical application. This study aims to evaluate the performance of an integrated methodology—based on a vine water consumption model and remote sensing data—to optimize the precision irrigation (PI) of a 100-ha commercial vineyard during two consecutive growing seasons. In addition, a cost-benefit analysis (CBA) was conducted of the tested strategy. Using an NDVI generated map, a vineyard with 52 irrigation sectors and the varieties *Tempranillo*, *Cabernet* and *Syrah* was classified in three categories (*Low*, *Medium* and *High*). The proposed methodology allowed viticulturists to adopt a precise RDI strategy, and, despite differences in water requirement between irrigation sectors, pre-defined stem water potential thresholds were not exceeded. In both years, the difference between maximum and minimum water applied in the different irrigation sectors varied by as much as 25.6%. Annual transpiration simulations showed ranges of 240.1–340.8 mm for 2016 and 298.6–366.9 mm for 2017. According to the CBA, total savings of 7090.00 € (2016) and 9960.00 € (2017) were obtained in the 100-ha vineyard with the PI strategy compared to not PI. After factoring in PI technology and labor costs of 5090 €, the net benefit was 20.0 € ha^{-1} in 2016 and 48.7 € ha^{-1} in 2017. The water consumption model adopted here to optimize PI is shown to enhance vineyard profitability, water use efficiency and yield.

Keywords Precision irrigation · Viticulture · Transpiration · Vine water consumption model · Stem water potential

---

J. Marsal—Passed away in 2017.

✉ J. Bellvert
  joaquim.bellvert@irta.cat

[1] Efficient Use of Water in Agriculture Program, Institute of AgriFood Research and Technology (IRTA), Parc Científic i Tecnològic Agroalimentari de Gardeny (PCiTAL), Fruitcentre, 25003 Lleida, Spain

Introduction

In viticulture, maximum incomes are not always achieved with maximum yield but by maintaining a certain balance between yield and berry composition. It is evident that judicious irrigation contributes to improving water use efficiency (WUE), controlling canopy vigor and enhancing grapevine berry composition (Chaves et al. 2007). In particular, the adoption of regulated deficit irrigation (RDI) strategies has been widely used in red grape varieties as a water saving strategy as well as to enhance berry composition attributes (Roby et al. 2004; Santesteban et al. 2011; Basile et al. 2011; Casassa et al. 2015). For instance, Basile et al. (2011) reported that in cv. 'Cabernet Sauvignon', berry composition improved when mild stress was applied between fruit set and veraison, and with moderate to severe water stress in post-veraison. The precise adoption of RDI requires careful selection of the moment, intensity and duration of the water deficit application (Conesa et al. 2018). This can only be properly achieved with a precise knowledge of the seasonal sensitivity of grapevine to water stress and using physiological plant-based tools such as the leaf/stem water potential as indicators of water stress (Girona et al. 2006, 2009). However, the main drawback when adopting these irrigation strategies in commercial vineyards is that it is extremely complicated to attain the same desired water stress level in all the subzones within a vineyard. The spatial differences in soil properties and topography reflect changes in water requirements across a vineyard, thereby limiting the efficient use of water. If irrigation is uniformly applied without considering spatial differences in water requirements there is a risk of a very significant productive and quality reduction in subzones where water stress is excessive. Equally, in overwatered subzones, the intended berry composition quality levels may not be achieved. To succeed with the practical application of RDI strategies at field level, it is first necessary to consider the following three aspects: (i) to characterize within-field soil spatial variability, since not all soils retain or provide water to the plant at the same rates. Currently, an appropriate procedure to map the spatial variation of soil properties is through the measurement of apparent soil electrical conductivity (EC_a), using electromagnetic induction conductivity instrumentation such as the commercial Veris 3100 sensor system (Veris Technologies, Salina, KS) or EM-38 sensors (Geonics Ltd., Mississauga, Ont, Canada) (Corwin and Lesch 2003; Abdy et al. 2008). Good correlations between EC_a and soil salinity, soil water content and soil texture have been widely reported (Moral et al. 2010; Uribeetxebarria et al. 2018); (ii) to adapt secondary irrigation networks according to the natural variability of soils. Several studies have proposed different methodologies to re-design the irrigation sectors based on yield map time-series, soil properties or spectral vegetation indices (Bellvert et al. 2012; Martínez-Casasnovas et al. 2009); and (iii) to obtain appropriate physiological knowledge about the optimal water stress thresholds of each variety and the optimal phenological moment to achieve the best balance between yield and berry composition.

Until now, the most commonly used irrigation practice by viticulturists has been based on a simple water balance approach, where crop evapotranspiration (ET_c) is calculated with standard crop coefficients (K_c) and the soil water content with data from soil moisture sensors, which are installed in a particular representative place of the vineyard. Then, irrigation scheduling is uniformly applied in the whole vineyard. Some large modernized wineries also complement this methodology with information gathered from other plant-based sensors (Jones 2004; Eastham and Gray 1998; Ginestar et al. 1998a, b). However, the use of any plant-based or similar indicator for scheduling irrigation requires the definition of reference or threshold values, beyond which irrigation is necessary. In addition, a

general limitation to plant-based methods is that they do not usually give information on 'how much' irrigation to apply at any one time, only on whether irrigation is needed or not (Jones 2004). Thus, irrigation prescriptions which use such tools when RDI is to be imposed have to be determined through trial and error methods.

The development of new precision irrigation (PI) scheduling systems aims to quantify the irrigation needs at spatial level according to the actual vine water status and with the goal of achieving a specific target. For this to be accomplished, the new challenge for PI in viticulture is to use a series of technological procedures in an integrated manner to individually resolve the three requirements described above for the implementation for RDI strategies, but which, without a clear link between them, cannot be commercially applied. Such new methodology needs to be properly integrated and can, for instance, be based on the use of geographic information systems (GIS), remote sensing, crop simulation models and irrigation management knowledge. These integrated procedures must also consider the criteria of the seasonal sensitivity of vines to water stress, and to have a reasonable cost/benefit ratio. A priori, the proper adoption of RDI strategies in red grape varieties seems profitable. According to the Raïmat winery (Spain), the difference in the rate of return between standard and high-quality berries can be as much as 310 € tn^{-1}. This means that in a vineyard with an average yield of 8–10 tn ha^{-1}, an income of 2700 € ha^{-1} can be obtained. In addition, improvements in water use efficiency (WUE) can also reduce water and electricity costs by up to 20%. If the actual average cost of energy and water is 320 € ha^{-1}, a potential saving of 20% corresponds to 64 € ha^{-1}.

In view of the above, the first objective of the present study was to develop a decision-oriented vine water consumption model for scheduling irrigation. This model has to be able to simulate the actual amount of water evapotranspirated per vine and to determine the necessary amount of water to be applied when different irrigation strategies (either full-irrigation or RDI) are to be imposed. The second objective was to demonstrate the performance of an integrated methodology for optimizing the precise irrigation of a 100-ha commercial vineyard based on use of the developed vine water consumption model and remote sensing data. Finally, a cost-benefit analysis (CBA) was performed to evaluate the profitability of conducting a PI management using the abovementioned integrated methodology.

It was hypothesized that the implementation of RDI in a 100-ha vineyard with notable differences in vine water requirements can only be successfully adopted with a series of integrated technological procedures based on the use of remote sensing as a tool to identify spatial variability and to classify irrigation sectors with similar characteristics, and a vine water consumption model capable to quantify irrigation needs according to actual and targeted vine water status. The proper adoption of this procedure could enhance vineyard profitability, water use efficiency and yield.

Materials and methods

Model description

The model developed in this study uses CropSyst principles (http://modeling.bsyse.wsu.edu/CS_Suite_4/CropSyst/index.html) (Stöckle et al. 2003) and has been recently adapted for different deciduous trees (Marsal et al. 2013, 2014). For this study, the water consumption model was adapted for grapevines and written in Matlab® language (MATLAB 2014b, The MathWorks, Inc., Natick, Massachusetts, United States) using experimental

empirical regression data obtained in previous studies. A diagram of the model with the interrelationships between the different parameters is shown in Fig. 1. Input parameters, such as weather, fraction of intercepted radiation (f_{IR}) and stem water potential (Ψ_{stem}), are introduced in the model in separate files. Since this model is run on a daily basis, daily weather data is required (maximum and minimum air temperature, maximum and minimum relative humidity, solar global radiation, rainfall and wind speed). Reference evapotranspiration (ET_o) (mm day^{-1}) estimation was calculated using the FAO Penman–Monteith equation (Allen et al. 1998).

The model allows the user to choose the irrigation strategy to be adopted throughout the growing season: (i) full irrigation (FI) or (ii) RDI. Irrigation prescriptions for FI are calculated based on ET estimates at full transpiring canopy. The stem water potential thresholds (Ψ_{thr}) can be defined at different phenological stages when an RDI strategy is adopted. The vegetative growth of the vine is determined as a function of the fraction of the canopy-intercepted solar radiation (f_{IR}), which can be either measured or simulated. Hourly f_{IR} is converted to daily f_{IR} (f_{IRd}) according to the model of Oyarzun et al. (2007). Canopy dimensions (i.e. height, width and length) and geographical coordinates of the vineyard are needed. If f_{IR} measurements are not available, the model can generate simulations of f_{IRd} using a polynomial function based on the accumulation of growing degree-days (GDD).

The phenological stages were defined based on GDD. The accumulation of GDD for each stage was determined with a modified version of the single triangle algorithm method (Zalom et al. 1983; Nendel 2010) described in Prats-Llinàs et al. (2020). The base and upper threshold temperatures were 4 °C and 26 °C, respectively. A maximum heat temperature threshold of 43 °C was also defined. On the occasions when the daily maximum temperature exceeded this threshold, the daily maximum temperature was corrected
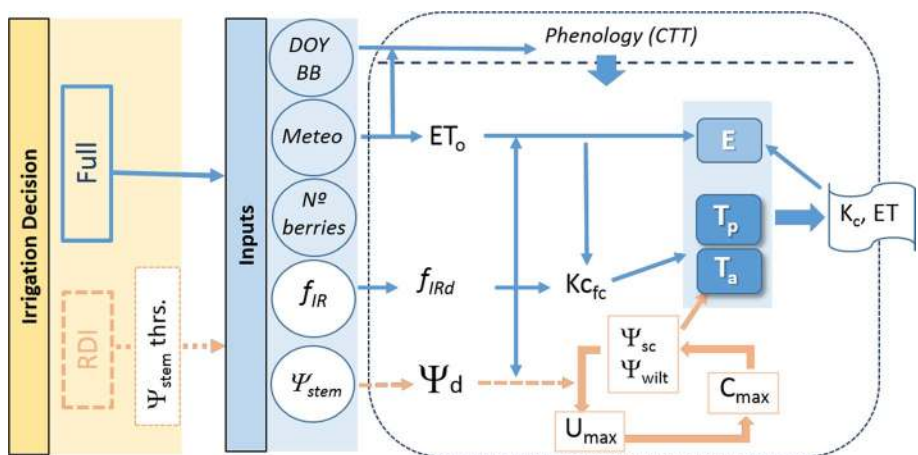
Fig. 1 Schematic representation of the interrelationship of the vine-water parameters of the vine water consumption model. *Full and RDI* full and regulated deficit irrigation strategies, respectively, *DOY BB* day of the year at bud-break, *Meteo* weather data, *no berries* number of berries per m^2, which, as default, is considered to be 900 berries m^{-2}, f_{IR} and f_{IRd} measured and daily fraction of canopy-intercepted radiation, respectively, Ψ_{stem} and Ψ_d midday and daily stem water potential, respectively, *CTT* cumulative thermal time, ET_o reference evapotranspiration, K_{cfc} full canopy crop coefficient, Ψ_{sc} and Ψ_{wilt} water potential that does not limit transpiration and at wilting point, respectively, C_{max} maximum vine hydraulic conductance; U_{max} maximum water uptake, T_p and T_a vine daily potential and actual transpiration, respectively, *E* soil evaporation, K_c irrigation crop coefficient

by applying the relationship between radiation use efficiency (RUE) and temperature described in Prats-Llinàs et al. (2020).

At any stage of canopy development, ET is separated into transpiration (T) and soil evaporation (E) components.

$$ET = T + E$$

Potential transpiration (T_p) (assuming total canopy cover at full transpiration) is calculated as:

$$T_p = \left(Kc_{fc}\left(f_{IRd}\right) ET_o + (- 0.10 + 0.13\ VPD)\right)$$

where Kc_{fc} represents the K_c for total canopy cover. In this modelling study, Kc_{fc} includes only vine transpiration and seasonal values were obtained from Picón-Toro et al. (2012) for a mature *cv. Tempranillo* vineyard as a function of f_{IRd} and thermal time from bud-break.

Soil evaporation (E) is calculated as:

$$E = K_e ET_o$$

where K_e represents the soil evaporation coefficient and was calculated using experimental data from microlysimeters and as a function of the amount of irrigation water applied in the previous irrigation event and f_{IRd}.

If an RDI strategy is adopted, then it is necessary to enter midday stem water potential (Ψ_{stem}) measurements into the model. Using this data, the model calculates the amount of water needed in order to reach the pre-defined Ψ_{thr}. Daily values of Ψ_{stem} (Ψ_d) were obtained as an integration of the diurnal course of Ψ_{stem} (every 2 h) measurements in TMP Low vines. An empirical polynomial relationship which related Ψ_{stem} with Ψ_d was developed ($R^2 = 0.86$; n = 40).

$$\psi_d = - 0.3186\psi_{stem}^2 + 0.2627\psi_{stem} - 0.2584$$

Maximum plant hydraulic conductance (C_{max}) can be calculated according to an analogue Ohm's law for full canopy cover as:

$$C_{max} = \frac{U_{max}}{\Psi_{fc} - \Psi_{sc}}$$

where U_{max} is a parameter of the model that represents the maximum water uptake of the crop, Ψ_{sc} is the lowest plant water potential that does not limit transpiration, and Ψ_{fc} is soil water potential at field capacity. Values for Ψ_{sc} change throughout the season, and those adopted in this study coincided with those Ψ_{stem} values that had a crop water stress index (CWSI) equal to zero (from $- 0.4$ to $- 1.1$ MPa) in the empirical regressions obtained by Bellvert et al. (2015) in different grapevine cultivars. Values of Ψ_{fc} were established at $- 0.033$ MPa. The percentage of reduction due to water stress was calculated as:

$$Reduction(\%) = 1 - \frac{\Psi_d - \Psi_{wilt}}{\Psi_{sc} - \Psi_{wilt}}$$

where Ψ_{wilt} is the lowest plant water potential at wilting point, when transpiration is null. In this study, values of Ψ_{wilt} coincide with a CWSI of one (from $- 1.1$ to $- 1.7$ MPa) (Bellvert et al. 2015).

Then, actual transpiration (T_a) and evapotranspiration (ET_a) can be estimated as:

$$T_a = T_p(1 - Reduction)$$

$$ET_a = (T_a + E)$$

Based on this, irrigation scheduling was performed on a weekly basis as:

$$\text{Water applied} = (ET - \text{rainfall})/0.95$$

where rainfall corresponded to that accumulated during the previous week, and 0.95 is the efficiency of a drip irrigation system.

Study site

The study was carried out during the growing seasons 2016 and 2017 in a 100-ha organic commercial vineyard located in Raïmat (41°39′50″N–0°30′27″E) (Lleida, Spain) (Fig. 2a). The vineyard consisted of 52 irrigation sectors ranging between 0.6 and 2.6 ha and planted with the varieties *Cabernet Sauvignon* (CAB) (38), *Tempranillo* (TMP) (12) and *Syrah* (SYR) (2). The area has a typical Mediterranean climate, with dry and hot summers and mild winters. Total rainfall for the growing period 30th March to 16th October was 163.7 mm and 149.8 mm for 2016 and 2017, respectively. The annual accumulated reference evapotranspiration (ET$_o$) was 1100 mm in 2016 and 1400 mm in 2017. The vineyard was planted in 2010 with a 1.6×2.5 m spacing distance. The soil texture was silty-loam and the effective soil depth was ~0.8 m. The canopy system was trained using vertical shoot
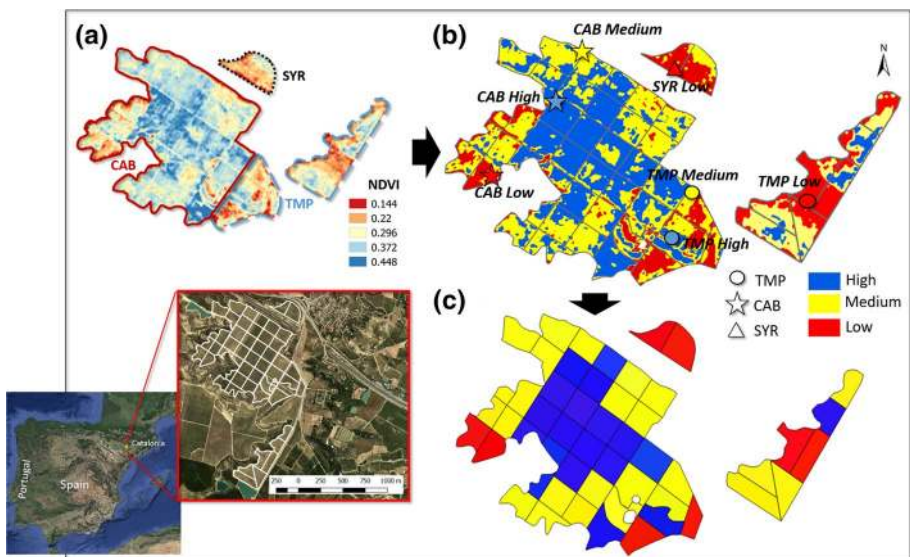
Fig. 2 Study area shown as: **a** location of the vineyard (41° 39′42.92″ N, 0° 30′59.48″ E), Lleida (Spain) with the distribution of different varieties and airborne-acquired high-resolution interpolated NDVI map from July 2015, **b** classification of the NDVI map into three categories: *High*, *Medium* and *Low* using a K-mean clustering analysis, and **c** irrigation sectors classified by category. Symbols indicate the location of the 'smart points'

positioning (VSP), with a bilateral, spur-pruned cordon located 1.0 m above the ground. Disease control and nutrition vine management were conducted following the wine grape production organic protocol of the 'Costers del Segre' Denomination of Origin (Catalonia, Spain) and the Catalan Council of Organic Agricultural Production (Catalan initials: CCPAE).

The spatial variability of the vineyard in terms of canopy vigor was determined in July of the 2015 growing season by using airborne high-resolution imagery. Zenith angle images were acquired with an aircraft equipped with a digital multispectral camera (DMSC), which integrates four independent narrow bandwidth spectral filters of 20 nm width (full-width, half-maximum) at the specific band center of 450 (blue), 550 (green), 680 (red), and 780 (near-infrared, NIR) nm. Image resolution is 2048×2048 pixel with 14-bit digitalization, with a 24–28 mm fixed focal length yielding an angular field of view (FOV) of 17°. Airborne images were acquired by SpecTerra Services Proprietary Limited (Perth, WA, Australia) under clear sky conditions at ~1500 m above ground level yielding images at 0.5 m spatial resolution. Post-flight image processing included a bidirectional reflectance distribution function (BRDF) correction for variations in the sun-sensor-target viewing geometry across each image. The SpecTerra proprietary BRDF correction algorithm preserved the spectral integrity within an image, but produced DN rather than absolute radiance. Therefore, the normalized difference vegetation index (NDVI) was calculated as:

$$NDVI = \frac{NIR - RED}{NIR + RED}$$

Pure vegetation and soil pixels were separated through a supervised classification algorithm. The ordinary kriging algorithm interpolation method was used to obtain NDVI maps, using only data from pure vegetation pixels. Then, a K-means clustering analysis was performed to classify NDVI spatial variability into three categories/clusters: Low, Medium and High (Fig. 2b). The ArcMap software (version 10.5 ESRI Inc. Redlands, ca., USA) was used to perform the spatial analysis.

Each irrigation sector was classified according to the predominant NDVI category (Fig. 2c). In addition, seven 'smart points', which visually corresponded to the most representative location by variety and NDVI category were also identified. These 'smart points' were classified as CAB (*High, Medium* and *Low*), TMP (*High, Medium* and *Low*) and SYR (*Low*). SYR was classified with only one category because the two irrigation sectors of this variety did not show spatial differences in NDVI. Each 'smart point' was composed of six vines, and vine physiological and structural measurements were conducted every one to two weeks and used as inputs of the crop model. The f_{IR} was measured using a portable ceptometer (Accupar Linear PAR, Decagon Devices, Inc., Pullman, WA, USA) placed in a horizontal position at ground level and perpendicular to vines. In order to cover vine spacing, five equally spaced measurements were taken on the shaded side of each vine. The incident radiation above the canopy was determined in an open space adjacent to each vine. Vine structural parameters such as height, and canopy width perpendicular to the row were also measured. Ψ_{stem} was measured at noon with a pressure chamber (model 3005; Soil Moisture Equipment Corp., Santa Barbara, ca., USA) according to the recommendations of McCutchan and Shackel (1992). Leaves were wrapped in plastic bags covered with aluminum foil at least one hour before Ψstem was measured. All measurements were taken in less than one hour with four leaves measured at each 'smart point'. Irrigation prescriptions were then conducted independently in each irrigation sector according to the model

outputs. Irrigation was scheduled on a weekly basis and distributed between three to four times a week. Drip emitters of 2.2 L h^{-1} were used, separated at 0.5 m. The volume of water applied was measured weekly using digital water meters (CZ2000-3M, Contazara, Zaragoza, Spain) located at each 'smart point'.

Definition of irrigation strategies

Irrigation scheduling consisted of adopting a RDI strategy for all wine grape varieties. For this purpose, different Ψ_{stem} thresholds were pre-defined by considering optimal Ψ_{stem} values obtained in previous studies in the same varieties (Girona et al. 2009; Basile et al. 2011). Table 1 shows a summary of the pre-defined Ψ_{stem} thresholds. Because, at the end of ripening, Syrah berries are more prone than the other varieties to display weight loss due to an insufficient compensation of transpirational water loss by xylem water uptake (Scharwies 2013), the pre-defined Ψ_{stem} values for that variety were slightly higher.

Evaluation of spatial variability and yield

The evaluation of vineyard spatial variability was performed on the basis of time-series Landsat-8 NDVI maps, which can be used to characterize canopy growth or vigor. A total of nine cloud-free images were downloaded from the Google Evapotranspiration Application EEFlux (https://eeflux-level1.appspot.com/), and processed each year (2015–2017) for the period April to end of August. Then, an ANOVA analysis was conducted with the averaged normalized difference vegetation index (NDVI) of each irrigation sector to assess spatial differences between irrigation sectors/categories and to evaluate the effect of conducting a differential irrigation management strategy during two consecutive years on canopy vigor heterogeneity. The fraction of reference ET (ETrF) was also downloaded from EEFlux for the same dates as NDVI. ETrF was obtained as the ratio of the computed instantaneous actual evapotranspiration (ET$_{inst}$) for each pixel and the evapotranspiration of a known reference crop (usually alfalfa for METRIC) using local meteorological observations. ET$_{inst}$ was obtained from the one-source energy balance model Mapping Evapotranspiration at high Resolution with Internalized Calibration (METRIC) (Allen et al. 2007). Some studies have shown a good agreement between yield and NDVI in vineyards (Martinez-Casasnovas et al. 2012; Sun et al. 2017). However, the lack of sensitivity of NDVI over leaf area index (LAI) higher than 2.0 (Towers et al. 2019) and the fact that high canopy vigor vines have more water demand and therefore could be more sensitive to water stress when water is scarce, it is possible that NDVI may not always be the best indicator

Table 1 Pre-defined midday stem water potential (Ψ_{stem}) thresholds for each variety and phenological stage

Year	Variety	Stage I (flowering to fruit set)	Stage II (fruit set to veraison)	Stage III (veraison to harvest)
2016	Cabernet (CAB)	− 0.6	− 0.7	− 1.2
	Tempranillo (TMP)			− 1.1
	Syrah (SYR)			− 1.0
2017	Cabernet (CAB)	− 0.6	− 0.8	− 1.2
	Tempranillo (TMP)		− 0.9	− 1.1
	Syrah (SYR)		− 0.8	− 1.0

for estimating yield. This study, evaluated NDVI and ETrF for the assessment of yield. Both seasonal average NDVI and ETrF of all irrigation sectors within the same category were averaged and regressed with yield. However, a preliminary step of that regression was to normalize the ETrF (ETrF$_{norm}$) using data of the three growing seasons. ETrF$_{norm}$ was then obtained as:

$$ETrF_{norm} = \frac{\overline{ETrF} - \overline{ETrF_{min}}}{\overline{ETrF_{max}} - \overline{ETrF_{min}}}$$

where $\overline{ETrF_{max}}$ and $\overline{ETrF_{min}}$ corresponded to seasonal averaged maximum and minimum values of ETrF for the three growing seasons.

On the other hand, this study also evaluated the feasibility of using estimates of the fraction of absorbed photosynthetically active radiation (FAPAR) obtained from the biophysical processor of the Sentinel Application Platform (SNAP) using Sentinel-2, as a replacement of in-situ f_{IR} measurements. The Sentinel-2 satellite system has multiple bands in the VISNIR spectral range, which can derive information of the biophysical parameters of the vegetation through radiative transfer models (RTM) at a spatial resolution of 10–20 m (Weiss and Baret 2016). Therefore, FAPAR estimates were validated with f_{IRd} throughout the 2017 growing season.

Harvesting was conducted on different dates and by zones when the accumulated total soluble solid concentration values reached the predefined levels established by the Raïmat winery.

Estimation of transpiration ratio, irrigation efficiency, and water productivity

Daily values of actual evapotranspiration (ET$_a$), transpiration (T$_a$), and yield for two seasons were used to compute the following parameters: (i) transpiration ratio (T$_a$/ET$_a$), (ii) irrigation efficiency (i.e.), calculated as the ratio between T$_a$ and the amount of water applied through irrigation and rainfall, and (iii) water productivity (WP) and agronomic water productivity (AWP), respectively calculated as the ratio between yield and T$_a$, and the ratio between yield and water applied (irrigation more rainfall).

Results and discussion

f_{IRd} and stem water potential

In all varieties and categories, f_{IRd} tended to increase sharply during the first part of the growing season, reaching maximum values of ~60% at DOY 200 (mid-July). From then, f_{IRd} remained stable for a while, as vegetative growth was controlled by pruning operations, before starting to decline until the end of the growing season (Fig. 3a–f). The seasonal pattern of f_{IRd} showed differences between varieties, categories and years. In 2016, the f_{IRd} of TMP was higher than the other two varieties (Fig. 3a–c). CAB and TMP also showed significant differences between categories, mostly occurring during phenological stages II and III. In both cases, cases the f_{IRd} of the *High* category tended to be higher than that of the other categories. In 2017, the f_{IRd} of all varieties increased considerably in comparison to the previous growing season, though the differences were greater in CAB and SYR than in TMP (Fig. 3d–f). It has been
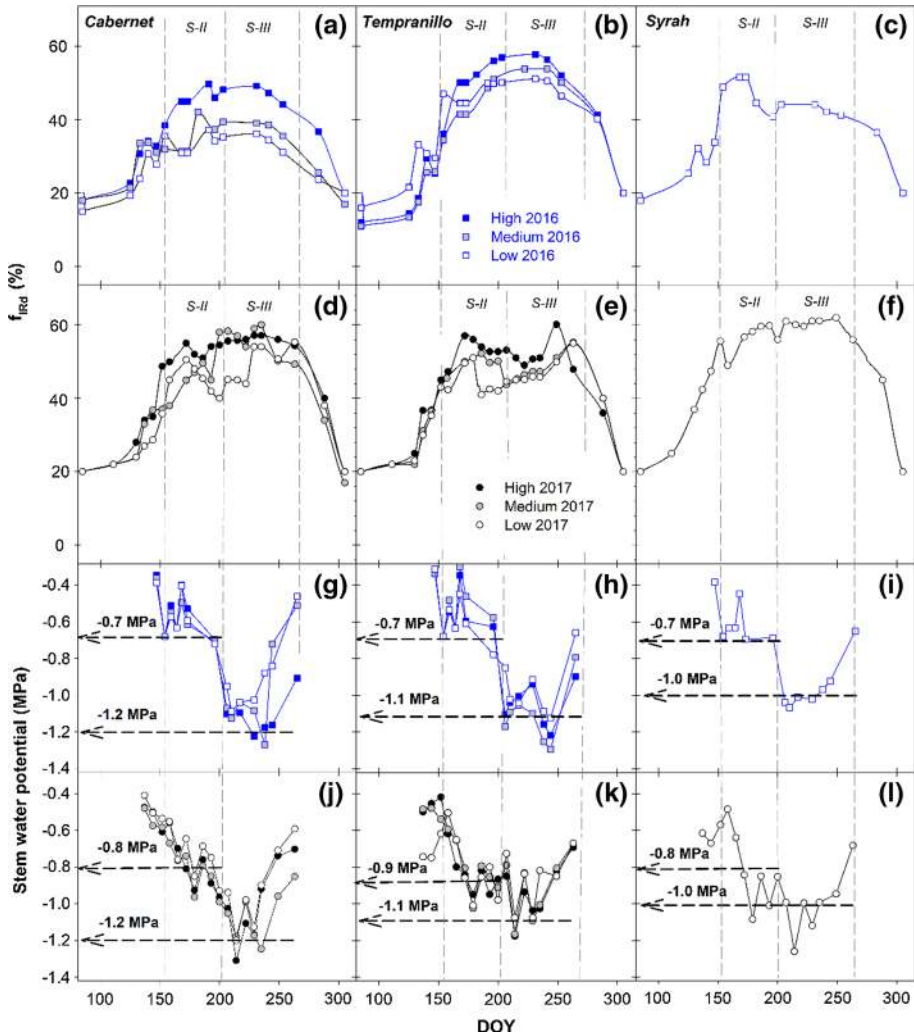
Fig. 3 Seasonal pattern of **a–f** daily fraction of canopy-intercepted radiation (f_{IRd}) and **g–l** midday stem water potential (Ψ_{stem}) measured at each 'smart point' during the growing seasons 2016 and 2017. Dashed arrows indicate the pre-defined Ψ_{stem} thresholds, and dashed lines the phenological stages

widely demonstrated that crop evapotranspiration (ET) is highly correlated with the fraction of light intercepted by the canopy (Ayars et al. 2003; Picón-Toro et al. 2012; Marsal et al. 2014). Consequently, differences in the abovementioned f_{IRd} estimate also reflected high variability within the vineyard in ET. However, Fig. 3g–l shows that, despite the differences in vine water requirements, Ψ_{stem} values followed the same trend in the three categories of each variety, and that, by conducting differential irrigation management, Ψ_{stem} values were maintained in accordance with the pre-defined Ψ_{stem} thresholds at the different phenological stages.

Seasonal pattern of vine transpiration and analysis of spatial variability

The actual transpiration (T_a) of vines at each 'smart point' was simulated during the whole growing season (Fig. 4). In each variety, simulations of T_a indicated significant differences among categories. The seasonal evolution of T_a followed the same pattern as that of vegetative growth, increasing from the beginning of the growing season until reaching maximum values of 4.0–5.5 mm day^{-1} when f_{IRd} also reached maximum values of 60% (~DOY 180). Subsequently, T_a started declining, in part due to the adoption of deficit irrigation during post-veraison. Overall, the highest T_a corresponded to vines of the category *High*, also coinciding with the highest f_{IRd}. Montoro et al. (2016) reported daily T_a rates in cv. *'Tempranillo'* comparable to those estimated in the present study. Other studies reported peak values of daily T_a of about 2.5 mm day^{-1} in vines with a canopy light interception of 30% (Intrigliolo et al. 2009). Assuming this canopy light interception was half of that measured in the current study, it confirms that this value was similar to those reported in the present study and which are shown in Fig. 4. In 2016, the highest accumulated T_a was for TMP, ranging from 313.6 mm to 340.8 mm depending on the category (*High*, *Medium* or *Low*). In 2016, SYR had similar values to *CAB High*, with accumulated T_a of 310.6 mm and 306.2 mm, respectively. In 2017, SYR had the highest accumulated T_a with 366.9 mm, while TMP and CAB had similar values in their respective categories ranging between 296.3 mm and 338.3 mm. Differences between vines in T_a measured at the different 'smart points' were calculated with the coefficient of variability (C_v), which ranged from 7.6–12.6%. Table 2 shows that accumulated T_a was about 15–22% lower than potential transpiration (T_p) over the whole growing season. RDI was mostly adopted during post-veraison (growth stage III), with the $CWSI_{SIII}$ showing accumulated water stress during that period which ranged from a minimum of 0.17 for *SYR Low* (2017) to a maximum of 0.36 for *CAB High*
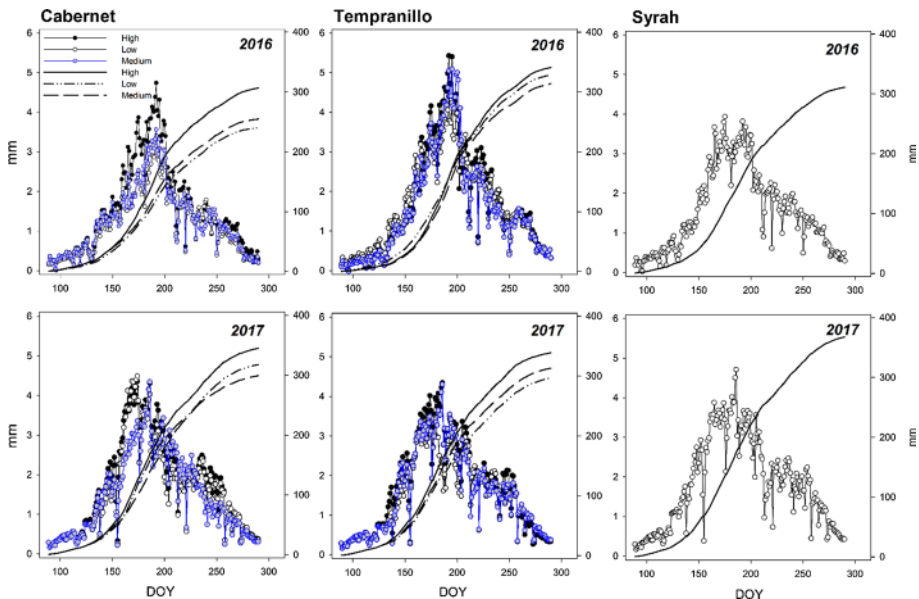
Fig. 4 Seasonal pattern of daily and accumulated actual transpiration (T_a) in each category of the varieties Cabernet Sauvignon, Tempranillo and Syrah during the growing seasons 2016 and 2017

Table 2 Summary of accumulated evapotranspiration components during the growing season and analysis of the effect of conducting a differential irrigation management strategy on spatial variability

	Year	T_p (mm)	T_a (mm)	E (mm)	ET_a (mm)	$CWSI_{All}$	$CWSI_{SIII}$	NDVI	C_v NDVI (%)	C_v NDVI (%)
CAB High	2015	–	–	–	–	–	–	0.62±0.02 a	22.5	31.1
CAB Medium		–	–	–	–	–	–	0.59±0.01 ab	29.1	
CAB Low		–	–	–	–	–	–	0.56±0.02 a	35.4	28.0
TMP High		–	–	–	–	–	–	0.65±0.00	–	
TMP Medium		–	–	–	–	–	–	0.62±0.01	35.1	
TMP Low		–	–	–	–	–	–	0.58±0.03	17.2	
SYR Low		–	–	–	–	–	–	0.53±0.08	16.9	16.9
CAB High	2016	377.6	306.2	97.5	403.7	0.19	0.36	0.54±0.01 a	17.2	27.5
CAB Medium		304.4	254.3	86.8	341.1	0.16	0.29	0.51±0.01 ab	27.7	
CAB Low		278.2	240.1	84.5	324.6	0.14	0.22	0.49±0.01 a	31.7	
TMP High		415.7	340.8	104.4	445.2	0.18	0.31	0.57±0.00	–	24.3
TMP Medium		376.6	313.6	97.3	410.9	0.17	0.32	0.54±0.01	33.0	
TMP Low		390.0	328.2	104.3	432.5	0.16	0.24	0.50±0.02	13.1	
SYR Low		365.7	310.6	100.4	411.0	0.15	0.22	0.49±0.02	9.4	9.4
CAB High	2017	401.3	328.8	98.9	427.7	0.18	0.28	0.57±0.02	29.2	28.3
CAB Medium		378.0	298.6	97.5	396.1	0.21	0.32	0.53±0.01	25.6	
CAB Low		367.8	317.2	102.5	419.7	0.14	0.22	0.54±0.01	29.5	
TMP High		409.9	338.3	107.1	445.4	0.17	0.22	0.54±0.00	–	26.1
TMP Medium		378.1	312.6	100.8	413.4	0.17	0.29	0.54±0.01	33.8	
TMP Low		352.8	296.3	98.7	395.0	0.16	0.17	0.48±0.01	8.3	
SYR Low		445.1	366.9	110.8	477.7	0.18	0.19	0.49±0.05	9.5	9.5
C_v 2015 (%)		–	–	–	–	–	–	6.8	32.0	
C_v 2016 (%)		13.7	13.7	8.2	11.5	10.7	19.5	6.2	28.6	
C_v 2017 (%)		7.9	7.6	4.8	6.9	12.6	23.1	6.1	28.4	

T_p and T_a are accumulated potential and actual simulated transpiration (mm), respectively; E is soil evaporation (mm), ET_a is actual evapotranspiration (mm), respectively. $CWSI_{All}$ and $CWSI_{SIII}$ correspond to water stress levels calculated as $1-(T_a/T_p)$ respectively for the entire growing season and growing stage III (post-veraison); NDVI was obtained from Landsat-8 through the EEFLUX platform. C_v is the coefficient of variability of the NDVI. Data is from the period 30th March (DOY 90) to 16th October (DOY 290). Rainfall for this period was 163.7 mm and 149.8 mm in 2016 and 2017, respectively. Different letters mean significant differences at $p \le 0.05$ using Tukey's honest significant difference test

(2016). The results also show that seasonal soil evaporation (E) accounted for 22–24% of total annual ET_a. Phogat et al. (2017) reported much higher evaporation values (44–59% of ET_a) using a subsurface drip irrigation system. However, the high differences in the amount of rainfall during the growing period between the two study sites may explain these dissimilarities. Other studies (Ferreira et al. 2012; Netzer et al. 2009; Cancela et al. 2012; Montoro et al. 2016) have shown seasonal evaporation varying from 7.4–30% of ET_a.

The averaged NDVI showed similar values among varieties/categories, ranging from 0.48 to 0.57 (Table 2). Significant differences between categories were only detected in CAB in 2015 and 2016. Other varieties showed non-significant slight differences in NDVI. These results do not fully agree with differences seen either with seasonal f_{IRd} or with the airborne high-resolution NDVI map acquired in 2015, where spatial differences between categories in each variety were more noticeable. In fact, the analysis of the coefficient of variation (C_v) of f_{IRd} during the whole growing seasons of 2016 and 2017 were 13% and 10%, respectively. Similar values were found for the airborne NDVI map, with a C_v of 15% between irrigation sectors. However, lower C_v values (6.2% and 6.1% in 2016 and 2017, respectively) were obtained when spatial differences were analyzed with Landsat-8 NDVI time-series (Table 2). One hypothesis is that these differences might be attributable to the coarse pixel size of the satellite imagery, which could soften the spatial differences in canopy vigor since it is also considering the effect of cover crop in the mid-row. In addition, it is important to take into account that spatial differences, when analyzed on a seasonal basis, are not as pronounced as when the analysis is conducted throughout a snapshot NDVI map acquired at the moment of maximum spatial differences in vegetative growth. Another hypothesis may be related with the saturation of NDVI for high f_{IR} values, thus avoiding that differences in f_{IR} could be detected from a certain threshold.

After two consecutive years of conducting differential irrigation management, the results also show that when analyzing the averaged C_v of NDVI of all the irrigation sectors of a given variety and comparing it with the previous year (2015), the C_v tended to decrease; from 31.1–28.3% in CAB, from 28.0–26.1% in TMP, and from 16.9–9.5% in SYR. Although these were not statistically significant differences, the trend indicates a slight reduction in canopy vigor heterogeneity among irrigation sectors, which can also influence berry composition.

Amount of water applied and cost-benefit analysis

In both 2016 and 2017, the amount of water applied varied between categories (Fig. 5). Overall, vines received more water in 2016 than in 2017, probably because the latter growing season had a higher rainfall and because the Ψ_{stem} reached more negative values during stage II. In 2016, the highest amount of water was applied in TMP, followed by CAB and SYR. In 2017, differences between varieties were not as clear, with SYR receiving the highest amount of water followed by TMP and CAB. These differences between varieties in terms of applied water agreed with the different pre-defined Ψ_{stem} thresholds. The coefficient of variation (C_v) of water applied in the different irrigation sectors was 10.6% in 2016 and 9.2% in 2017. The difference between maximum and minimum amount of water applied was 84.1 mm (2016) and 79.8 mm (2017), which in both years represents a difference of 25.6% in the amount of water applied. On the other hand, when the data is analyzed considering differences between categories within each variety, the highest variations were in 2017, with differences of 34.8 mm and 26.3 mm for CAB and TMP, respectively. These differences respectively correspond to water reductions of 13.0% and 9.0% for CAB
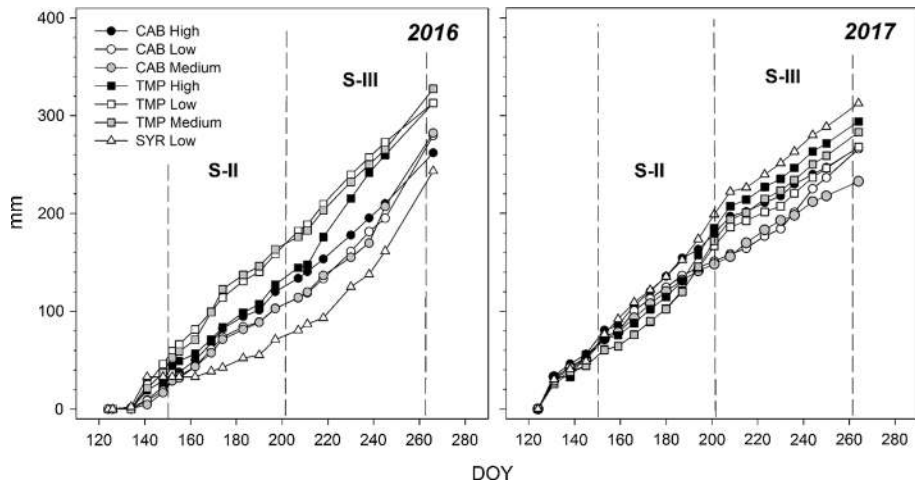
Fig. 5 Seasonal variation in cumulative water applied for each variety and category in the growing seasons 2016 and 2017. Dashed lines indicate dates that separates phenological stages II (fruit set to veraison) and III (veraison to harvest)

and TMP, respectively. Such significant water savings highlight the importance of conducting differential and precision irrigation management according to the differences in water requirements between irrigation sectors.

Although Ψ_{stem} has been commonly used in research and its advantages extensively demonstrated (Shackel et al. 1997; Girona et al. 2006; Williams 2017), commercial use of this technique is still limited, with only a few wineries currently using this tool in their protocols for scheduling irrigation. The main shortcomings are the initial investment cost and the time that is required to conduct a high number of measurements at midday in order to have a good representation of the vine water status of a whole vineyard. However, the present study demonstrates that, by taking advantage of remote sensing, it is possible to map the spatial variability of a vineyard, to identify zones and irrigation sectors with similar characteristics and to geolocate representative vines within each zone for collection of Ψ_{stem} and f_{IRd} measurements. By integrating this information into the developed vine water consumption model, this study has demonstrated that it is possible to conduct effective precision irrigation (PI) management. However, the costs and benefits of applying this methodology only during two consecutive years are still uncertain. Table 3 shows a cost-benefit analysis (CBA) which evaluates the feasibility of using the proposed methodology of the present study in a 100-ha vineyard. To achieve it, the PI management adopted in this study was compared against a not precision irrigation (NPI). The NPI simulated the irrigation prescriptions that a viticulturist should adopt to follow a full-irrigation strategy uniformly applied for the entire vineyard. Therefore, irrigation prescriptions were calculated with the vine water consumption model based on ET estimates at full transpiring canopy (Table 4).

The total fixed costs for scheduling irrigation based on a PI management system were found to be 5090 €. The biggest contributors to the fixed costs were the image acquisition with airborne, which accounted for 39.3% of fixed cost. However, this cost can be significantly reduced with the use of Sentinel-2 open-access data. The equipment recovery costs (calculated on a 10-year amortization plan) accounted for about 16% of fixed costs. The results indicate that the adoption of PI management in a 100-ha vineyard resulted in

Table 3 Costs for conducting a precision irrigation (PI) management in the 100-ha vineyard by operating the developed system

Concept		Cost (€ 100 ha^{-1})
Costs of obtaining NDVI map[a]		2000
Cost image processing & location of 'smart points'	7 h day^{-1} × 1 day × 20 € h^{-1}	140
Purchase: pressure chamber[b]	4500 €	450[c]
Purchase: ceptometer AccuPAR-80	3600 €	360[d]
Ψ_{stem} and f_{IRd} measurements	4 hours day^{-1} × 15 days × 20 € h^{-1}	1200
Costs of gasoline	2 L day^{-1} × 15 days × 1.33 € L^{-1}	40
Cost of the crop model: charge fees and maintenance[e]	3 € ha^{-1}	300
Trained technician for running the model[f]	2 h day^{-1} × 15 days × 20 € h^{-1}	600
Total		5090

[a]Actual cost of acquiring an NDVI map of 100-ha with an airborne platform is 20 € ha^{-1} (price of the Spanish company Agropixel). However, currently satellite imagery (i.e. PlanetLab or Sentinel-2) offers the possibility to obtain NDVI maps at spatial resolutions of 3–10 m for 5 € ha^{-1} or through open-access

[b]Cost of the SF-Pres35 (similar to Scholander) (Solfranc Tecnologias, SL)

[c,d]Amortization of the equipment was calculated on a 10-year basis

[e]Tentative price related to fees that a company or viticulturist would pay for using the model

[f]It has been taken into account that the average cost of an IRTA technician capable of conducting these functions is 20 € hour^{-1}

consumption of 0.26 hm^3 and 0.28 hm^3 of water in 2017 and 2016, respectively. These amounts represent, respectively, a total cost of 188.0 € ha^{-1} and 203.0 € ha^{-1}, of which 69% is related to the cost of the water itself and 31% to power consumption. Depending on year and category, between 14% and 38% less water was needed in the vineyard when a PI strategy was adopted compared to a NPI strategy. Generally, these differences were more evident in 2017 than in 2016 because in 2017 vines had a higher f_{IRd} and therefore a higher water demand. The total amount of water needed for uniform irrigation of a 100-ha vineyard under an NPI strategy was 0.38 hm^3 in 2016 and 0.40 hm^3 in 2017. These amounts represent energy and water costs of 273.9 € ha^{-1} and 288.2 € ha^{-1}, respectively, which are 35% and 53% higher than those calculated for the PI strategy. In total, the saving costs of conducting a PI strategy in the 100-ha amount to 7090.0 € and 9960.0 € in 2016 and 2017 respectively. However, since the associated technology and labor costs needed to establish this management strategy were 5090 €, the net benefit for the 100-ha was 2000 € in 2016 and 4870 € in 2017. This means that PI can be profitable in the first year of implementation. One of the main advantages of adopting PI is that fewer irrigation hours are required compared to NPI, and therefore these can be scheduled during the hours of the day when the electricity price is lowest (usually during the night), with a consequent further reduction in energy costs. It is also important to mention that this net benefit will rise with the number of hectares that are being managed, and that a further increase will be obtained once the 10-year term amortization for the purchased equipment has concluded. In addition, the benefits that can be obtained in terms of improvement in berry quality when an RDI is properly adopted should also be considered; according to the Raïmat winery, the difference in the rate of return between standard and high-quality berries can be as much as 310 € tn^{-1}.

Table 4 Comparative cost-benefit analysis (CBA) of irrigating a 100-ha vineyard using two different irrigation strategies: (i) precision irrigation (PI) management based on Ψ_{stem} thresholds and adopting RDI (actual data of this study), (ii) not precision-irrigation (NPI), where water is applied uniformly throughout the vineyard by simulating a full-irrigation strategy

	CAB high	CAB medium	CAB low	TMP high	TMP medium	TMP low	SYR low
Area (ha)	36.4	28.8	5.8	3.3	6.8	14.9	3.9
Precision irrigation (PI)							
Water applied 2016 (mm)	262.0	282.3	279.8	312.9	327.5	313.0	243.5
Water applied 2017 (mm)	267.5	232.7	266.1	294.1	283.2	267.8	312.5
Not precision irrigation (NPI)							
Water applied 2016 (mm)	359.1	351.7	323.7	439.7	400.6	407.8	381.3
Average 2016 (mm)	380.6						
Water applied 2017 (mm)	404.8	379.5	361.0	414.7	397.2	369.8	474.9
Average 2017 (mm)	399.5						

Costs (100-ha)	PI 2016	NPI 2016	PI 2017	NPI 2017
hm^3 water applied	0.28	0.38	0.26	0.40
Total kWh used	56390.6	76110	52223.2	79900.0
€ energy	6202.9	8372.1	5744.6	8789.0
€ water	14097.6	19027.5	13055.8	19975.0
Total €	20300.6	27399.6	18800.3	28764.0
€ ha^{-1}	203.0	273.9	188.0	287.6
Savings (€ ha^{-1})	70.9		99.6	
Savings (€ 100 ha^{-1})	7090.0		9960.0	

Maps of transpiration ratio, irrigation efficiency, water productivity and yield

Transpiration ratio, computed in the present study as the ratio between T_a and ET_a, varied slightly from 0.74 to 0.77 (Fig. 6a, b). Although T_a/ET_a did not show much variation between the different irrigation sectors, the most notable differences were seen in the irrigation sectors of TMP in 2016, with slightly higher T_a/ET_a values than in the other irrigation sectors. These values also illustrate the accumulated seasonal water losses through evaporation which, as previously mentioned, accounted for 22–24% of ET_a. The irrigation efficiency (IE) of the whole vineyard ranged from 0.58 to 0.83 in 2016 and from 0.69 to 0.81 in 2017 (Fig. 6c, d). Generally, lower IE values were obtained in 2016 compared to 2017, probably because of the higher rainfall and, particularly in CAB 2016, because of lower accumulated seasonal T_a. Rainfall or irrigation water that is not transpired by the vine can be lost through evaporation or stored in the soil. In fact, the IE results illustrated an agreement between irrigation sectors with high IE values and irrigation sectors with low soil evaporation or high T_a/ET_a. Interestingly, water productivity (WP) varied non-significantly in a range from 2.56 to 5.64 kg m^{-3}, with the partial exception of TMP in 2016, which reached maximum values of 6.54–6.61 kg m^{-3} (Fig. 6e, f). Due to the problems
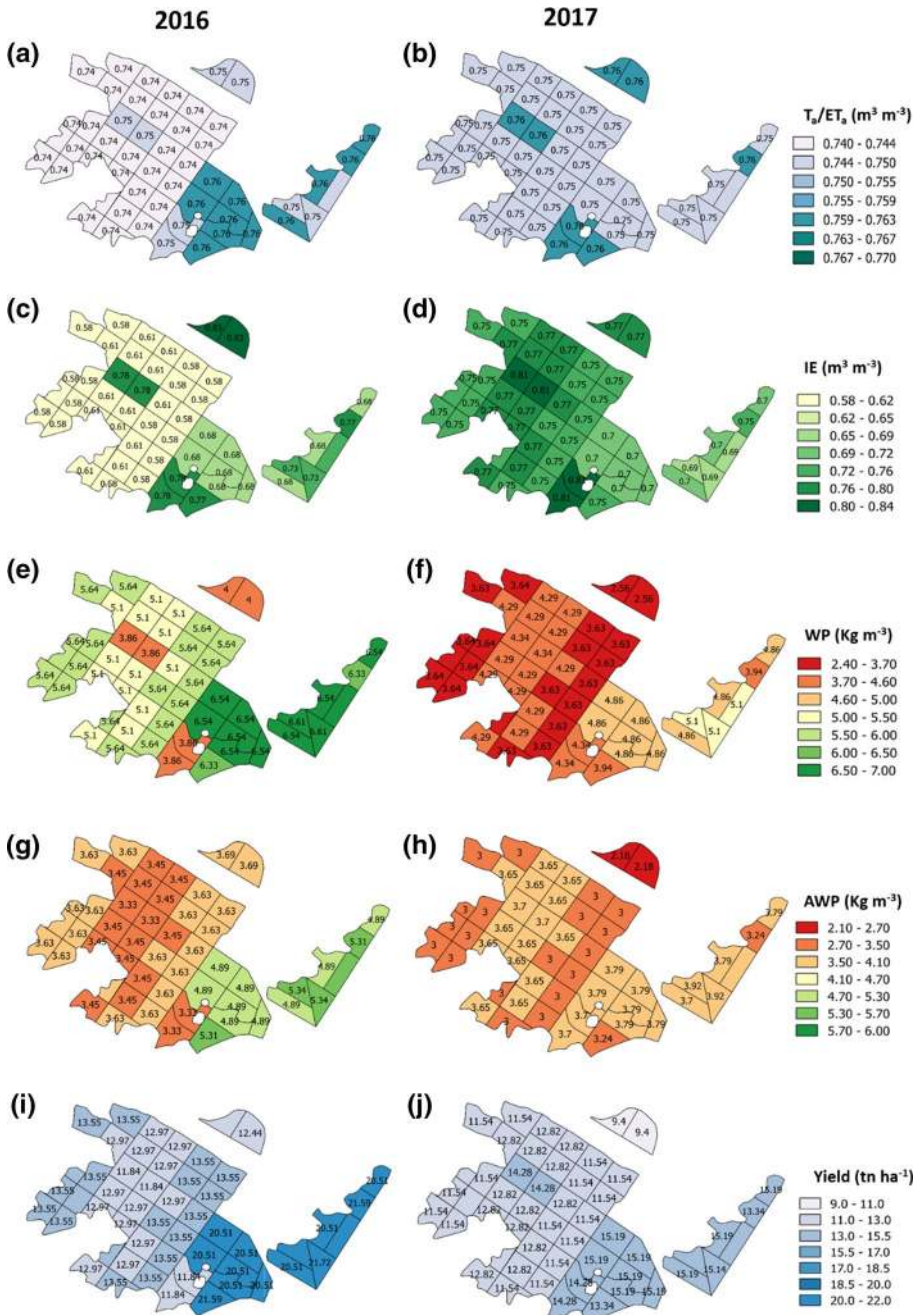
Fig. 6 Seasonal maps of **a**, **b** transpiration ratio (T_a/ET_a), **c**, **d** irrigation efficiency (IE) (T_a/irrigation water applied + rainfall), **e**, **f** water productivity (WP) (kg of yield/T_a), **g**, **h** agronomic water productivity (WP) (Kg of yield/irrigation water applied + rainfall), and **i**, **j** yield (tones ha^{-1}) for each irrigation sector of the vineyard, for the growing seasons 2016 and 2017

involved in estimating the component T_a, it is difficult to find studies in the literature that calculate vineyard WP as the ratio of yield/T_a. Among publicly available studies, only Phogat et al. (2017) has reported WP as yield/T_a, with values in a range of 11.2–13.5 kg m^{-3} for Chardonnay wine grapes. These values are higher than those observed in the present study. However, the difference may be strongly influenced by the seasonal accumulated transpiration, which in the study reported by Phogat et al. (2017) was approximately twice as high as that estimated in this study. Most of the published studies refer to WP as the yield per unit of water used in evapotranspiration (Kijne et al. 2003; Fereres and Soriano 2007) or applied through irrigation + rainfall (Egea et al. 2010; Ghrab et al. 2013; Mirás-Avalos et al. 2016). In the present study, WP calculated based on this definition was named as agronomic water productivity (AWP) and it ranged from 2.18 kg m^{-3} (SYR in 2017) to 5.34 kg m^{-3} (TMP in 2016) (Fig. 6g, h). These values agree with WP values in other studies of 2.4 kg m^{-3} (Texeira et al. 2009) and 3.4 kg m^{-3} (Atroosh et al. 2013), whereas a study in Chile reported WP values of 4.1–7.3 kg m^{-3} depending on the irrigation strategy employed (Zuñiga et al. 2018). However, this wide variability in the reported WP values is strongly influenced by differences in canopy management and cluster thinning, environmental conditions and rootstock variety.

Yield estimates

Using both satellite and airborne imagery, significant correlations between spectral vegetation indices and grape yield have been reported in some studies (Sun et al. 2017; Bellvert et al. 2012), but not in others (Bonilla et al. 2015, Anastasiou et al. 2018). In the present study, no statistically significant correlation was obtained in the regression between NDVI and yield (Fig. 7a). For a given range of NDVI values, yield varied in the range 7–22 tn ha^{-1}. These inconsistencies could be attributable to several causes: (i) it is widely acknowledged that yield is a function of transpiration, and that the latter increases as f_{IRd} increases (Suay et al. 2003). However, this is only true under potential conditions. When water stress occurs, it is because the demand for water exceeds the available amount of water. Thus, it
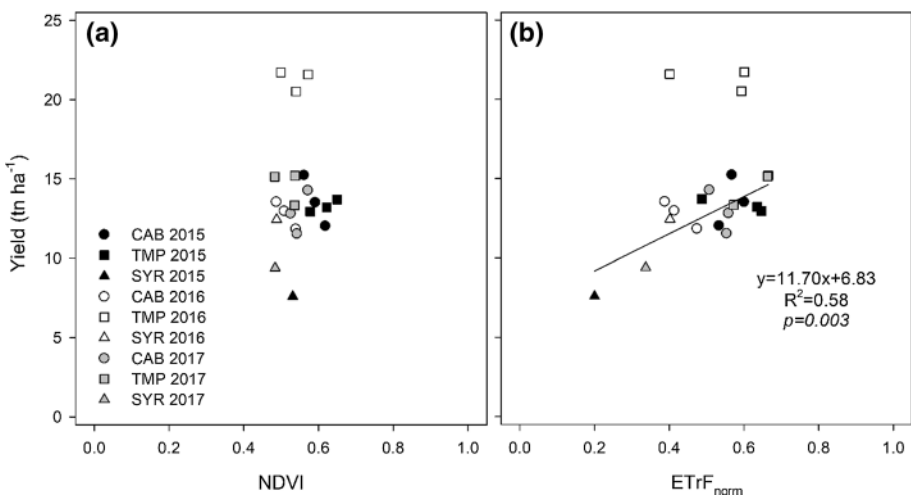

Fig. 7 Relationship between yield and **a** seasonal averaged NDVI and **b** the normalized fraction of reference evapotranspiration (ETrF$_{norm}$), both obtained from Landsat-8 images

is possible that despite having vines with high canopy vigor (higher water demand), if the amount of water applied is below the water demand, vines can be stressed and therefore have a negative impact on yield; (ii) the spectral vegetation index NDVI has been widely used to identify the spatial and temporal differences in vegetative growth in wine grapes (Balbontín et al. 2017; Sun et al. 2017). However, it is well documented that NDVI tends to saturate at high leaf area index (LAI) values (Barrett and Curtis 1999, Haboudane et al. 2004), resulting therefore in a restriction for quantifying vegetative growth, particularly in relatively dense canopies. In addition, Guillén-Climent et al. (2012) reported the high sensitivity of NDVI to soil background, percentage cover, and sun geometry in heterogeneous orchard canopies. The high sensitivity of NDVI to leaf pigments, spacing distance and training systems also needs to be taken into consideration. Therefore, no unique relationship between NDVI and LAI is universally applicable, and numerous parameters need to be taken into account in order to obtain accurate estimates of LAI. As previously mentioned, yield is a function of crop transpiration. In this respect, Fig. 7b shows a good positive relationship between yield and ETrF_norm for all points except for those of TMP in 2016 which, for a given level of ETrF_norm, tended to have a higher yield. These differences in yield could be attributable to a varying number of clusters as the result of differential cluster thinning.

Regression between FAPAR and f_{IRd}

A significant correlation was found between f_{IRd} and FAPAR_S2, with a coefficient of determination (R^2) of 0.30 and an RMSE of 0.10 (Fig. 8). Data used in that regression corresponded to the period 15th May to 8th October. Data outside this period was not considered because the presence of inter-row grass cover crop negatively affected the correct estimates of FAPAR_S2. Although the initial results were significant and the estimates of FAPAR_S2 could probably be used as an alternative to *in situ* f_{IRd} measurement, further research is needed to validate it in heterogeneous crops. FAPAR_S2 is first obtained from radiative transfer models, which depends on canopy structure, vegetation element optical properties and illumination conditions. After, it is used to train a neural network which produces in parallel estimates of the considered biophysical variables. Further research should be focus to train the neural network in vines with different row orientations and training

Fig. 8 Regression between the simulated daily fraction of intercepted radiation (f_{IRd}) and the fraction of absorbed photosynthetically active radiation (FAPAR) obtained from the Sentinel-2 biophysical processor of the SNAP platform during the growing season 2017
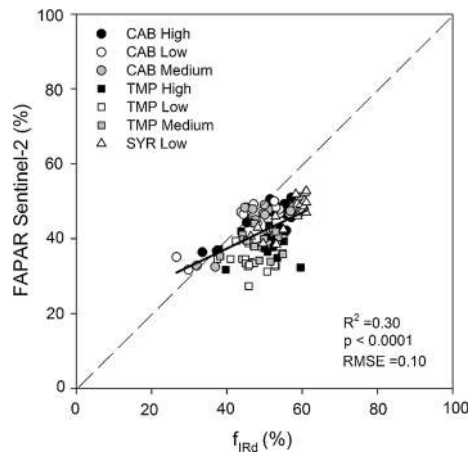
systems. Since most of the cost for conducting a PI management is related to Ψ_{stem} and f_{IR} measurements (Table 3), spatio-temporal estimates of FAPAR would considerably reduce the cost and to improve the chances to conduct a PI management.

Conclusions

This study demonstrates the technical and economic feasibility of developing a precision irrigation management strategy for a 100-ha organic vineyard using the technological procedure of a decision-oriented vine water consumption model and remote sensing information. Despite the heterogeneity in vine water consumption between the different irrigation sectors of the vineyard, scheduling irrigation in a differential manner according to the prescriptions generated by the vine water consumption model resulted in vines with similar vine water status in all the irrigation sectors and throughout the growing season. In both years of the study, the difference between the maximum and the minimum amount of water applied in the different irrigation sectors varied by as much as 25.6%. The water savings that were achieved increased both water and energy use efficiency. When comparing a PI with a NPI strategy in terms of the amount of water needed in the vineyard, differences ranged between 14% and 38% depending on the year and water demand of the irrigation sector. Energy and water cost savings as high as 35% and 53%, respectively, were obtained with the precision irrigation strategy. It is estimated that the net economic benefit to the farmer (related to water and energy) of conducting a precision irrigation management strategy, after including all overhead expenses, amounted to 20.0 € ha^{-1} in 2016 and 48.7 € ha^{-1} in 2017. After two consecutive years of differential irrigation management, the coefficient of variability (C_v) of NDVI between irrigation sectors showed a slight declining trend, with values falling from 32.0% in 2015 to 28.4% in 2017, indicating greater homogeneity within the vineyard. It therefore seems reasonable to conclude that—taking into account the demonstrated net energy and water savings and consequent economic benefit, the associated improvement in berry composition attributes due to the adoption of RDI, as well as the trend of increased homogeneity—the adoption of PI is both necessary and profitable for most wineries. The transpiration ratio, i.e., WP and AWP of the vineyard ranged from 0.74 to 0.76 m^3 m^{-3}, 0.58–0.83 m^3 m^{-3}, 2.56–6.61 kg m^{-3} and from 2.18 to 5.34 kg m^{-3} respectively. The seasonal soil evaporation (E) accounted for 22–24% of the total amount of evapotranspiration (ET$_a$). Yield was positively correlated to the fraction of reference evapotranspiration (ETrF$_{norm}$), but not with the NDVI. Finally, although more research is needed in this respect, it seems that the use of estimations of the biophysical parameters of the vegetation (i.e. FAPAR) using the S2 toolbox of the SNAP software could be a feasible alternative to obtaining time-series of canopy vegetative growth at spatial level, and as a consequence it will help the reduce costs related to measurements in the vines.

References

Abdy, H., Robinson, D. A., Seyfried, M., & Jones, S. B. (2008). Geophysical imaging of watershed sub-surface patterns and prediction of soil texture and water holding capacity. *Water Resources Research, 44*(4), 18.

Allen, R. G., Pereira, L. S., Raes, D., & Smith, M. (1998). *Crop evapotranspiration—guidelines for computing crop water requirements*. Rome: FAO Irrigation and drainage paper 56. Food and Agriculture Organization.

Allen, R. G., Tasumi, M., & Trezza, R. (2007). Satellite-Based Energy balance for Mapping Evapotranspiration with internalized calibration (METRIC)—model. *Journal of Irrigation and Drainage Engineering, 133*(4), 380–394.

Anastasiou, E., Balafaoutis, A., Darra, N., Psiroukis, V., Biniari, A., Xanthopoulus, G., & Fountas, S. (2018). Satellite and proximal sensing to estimate the yield and quality of table grapes. *Agriculture, 8*, 94.

Atroosh, K. B., Mukred, A. W. O., & Moustafa, A. T. (2013). Water requirement of grape (Vitis vinifera) in the Northern Highlands of Yemen. *Journal of Agricultural Science, 5*(4), 136–145.

Ayars, J. E., Johnson, R. S., Phene, C. J., Trout, T. J., Clark, D. A., & Mead, R. M. (2003). Water use by drip-irrigated late-season peaches. *Irrigation Science, 22*, 187–194.

Balbontín, C., Campos, I., Odi-Lara, M., Ibacache, A., & Calera, A. (2017). Irrigation performance assessment in table grape using the reflectance-based crop coefficient. *Remote Sensing, 9*, 1276.

Barrett, E. C., & Curtis, L. F. (1999) Introduction to environmental remote sensing (Stanley Thornes: Cheltenham) (pp. 323–346). https://doi.org/10.4324/9780203761038.

Basile, B., Marsal, J., Mata, M., Vallverdú, X., Bellvert, J., & Girona, J. (2011). Phenological sensitivity of Cabernet Sauvignon to water stress: Vine physiology and Berry composition. *American Journal Enology and Viticulture, 62*(4), 452–461.

Bellvert, J., Marsal, J., Mata, M., & Girona, J. (2012). Identifying irrigation zones across a 7.5-ha 'Pinotnoir' vineyard based on the variability of vine water status and multispectral images. *Irrigation Science, 30*, 499–509.

Bellvert, J., Zarco-Tejada, P. J., Girona, J., Marsal, J., & Fereres, E. (2015). Seasonal evolution of crop water stress index in grapevine varieties determined with high resolution remote sensing thermal imagery. *Irrigation Science, 33*, 81–93.

Bonilla, I., Martinez de Toda, F., & Martínez-Casasnovas, J. A. (2015). Vine vigor, yield and grape quality assessment by airborne remote sensing over three years: Analysis of unexpected relationships in cv. Tempranillo. *Spanish Journal of Agricultural Research, 13*(2), e0903.

Cancela, J. J., Fandiño, M., Rey, B. J., Rosa, R., & Pereira, L. S. (2012) Estimating transpiration and soil evaporation of vineyards from the fraction of ground cover and crop height—application to 'Albariño' vineyards of Galicia. In *Proc. XXVIIIth IHC-IS Viti&Climate: Effects of Climate Change on Production and Quality of Grapevines and Their Products. Acta Horticulturae on* 931 (pp. 227–234).

Casassa, L. F., Keller, M., & Harbertson, J. F. (2015). Regulated deficit irrigation alters anthocyanins, tannins and sensory properties of Cabernet Sauvignon Grapes and wines. *Molecules, 20*, 7820–7844.

Chaves, M. M., Santos, T. P., Souza, C. R., Ortuño, M. F., Rodrigues, M. L., Lopes, C. M., Maroco, J. P., & Pereira, J. S. (2007). Deficit irrigation in grapevine improves water-use efficiency while controlling vigour and production quality. *Annals of Applied Biology, 150*, 232–252.

Conesa, M. R., de la Rosa, J. M., Fernández-Trujillo, J. P., Domingo, R., & Pérez-Pastor, A. (2018). Deficit irrigation in commercial mandarin trees: Water relations, yield and quality responses at harvest and after cold storage. *Spanish Journal of Agricultural Research, 16*, 3.

Corwin, D. L., & Lesch, S. M. (2003). Application of soil electrical conductivity to precision agriculture: Theory, principles, and guidelines. *Agronomy Journal, 95*(3), 455–471.

Eastham, J., & Gray, S. A. (1998). A preliminary evaluation of the suitability of sap flow sensors for use in scheduling vineyard irrigation. *American Journal of Enology and Viticulture, 49*, 171–176.

Egea, G., Nortes, P. A., González-Real, M. M., Baille, A., & Domingo, R. (2010). Agronomic response and water productivity of almond trees under contrasted deficit irrigation regimes. *Agricultural Water Management, 97*, 171–181.

Fereres, E., & Soriano, M. A. (2007). Deficit irrigation for reducing agricultural water use. *Journal of Experimental Botany, 58*, 147–159.

Ferreira, M. I., Slivestre, J., Conceicao, N., & Malheiro, A. C. (2012). Crop and stress coefficients in rainfed and deficit irrigation vineyards using sap flow techniques. *Irrigation Science, 30*, 433–447.

Ghrab, M., Zitouna, R., Mimoun, M. B., Masmoudi, M. M., & Mechlia, N. B. (2013). Yield and water productivity of peach trees under continuous deficit irrigation and high evaporative demand. *Biological Agriculture & Horticulture, 29*(1), 29–37.

Ginestar, C., Eastham, J., Gray, S., & Iland, P. (1998a). Use of sap-flow sensors to schedule vineyard irrigation. I. Effects of post-veraison water deficits on water relations, vine growth, and yield of Shiraz grapevines. *American Journal of Enology and Viticulture, 49*, 413–420.

Ginestar, C., Eastham, J., Gray, S., & Iland, P. (1998b). Use of sap-flow sensors to schedule vineyard irrigation. II. Effects of post-veraison water deficits on composition of Shiraz grapes. *American Journal of Enology and Viticulture, 49*, 421–428.

Girona, J., Marsal, J., Mata, M., Del Campo, J., & Basile, B. (2009). Phenological sensitivity of berry growth and composition of Tempranillo grapevines (*Vitis Vinifera* L.) to water stress. *Australian Journal Grape & Wine Research, 15,* 268–277.

Girona, J., Mata, M., del Campo, J., Arbonés, A., Bartra, E., & Marsal, J. (2006). The use of midday leaf water potential for scheduling deficit irrigation in vineyards. *Irrigation Science, 24*, 115–127.

Guillén-Climent, M. L., Zarco-Tejada, P. J., & Villalobos, F. J. (2012). Estimating radiation interception in an olive orchard using physical models and multispectral airborne imagery. *Israel Journal of Plant Sciences, 60*, 107–121.

Haboudane, D., Miller, J. R., Pattey, E., Zarco-Tejada, P. J., & Strachan, I. B. (2004). Hyperspectral vegetation indices and novel algorithms for predicting green LAI of crop canopies: Modeling and validation in the context of precision agriculture. *Remote Sensing of Environment, 90*, 337–352.

Intrigliolo, D. S., Lakso, A. N., & Piccioni, R. M. (2009). Grapevine cv. 'Riesling' water use in the northeastern United States. *Irrigation Science, 27*, 253–262.

Jones, H. (2004). Irrigation scheduling: advantages and pitfalls of plant-based methods. *Journal of Experimental Botany, 55*, 407.

Kijne, J. W., Barker, R., & Molden, D. J. (2003). *Water productivity in agriculture: Limits and opportunities for improvement* (Vol. 19, p. 332) Wallingford, UK: CABI, International Water Management Institute (IWMI)

Marsal, J., Girona, J., Casadesus, J., Lopez, G., & Stöckle, C. O. (2013). Crop coefficient (Kc) for apple: Comparison between measurements by a weighing lysimeter and prediction by CropSyst. *Irrigation Science, 31,* 455–463.

Marsal, J., Johnson, S., Casadesús, J., Lopez, G., Girona, J., & Stöckle, C. (2014). Fraction of canopy intercepted radiation relates differently with crop coefficient depending on the season and the fruit species. *Agricultural and Forest Meteorology, 184*, 1–11.

Martinez-Casasnovas, J. A., Agelet-Fernandez, J., Arnó, J., & Ramos, M. C. (2012). Analysis of vineyard differential management zones and relation to vine development, grape maturity and quality. *Spanish Journal of Agricultural Research, 10*(2), 326–337.

Martínez-Casasnovas, J. A., Vallés, D., & Ramos, M. C. (2009). Irrigation management zones for precision viticulture according to intra-field variability. In A. Bregt, S. Wolfert, J. E. Wien, & C. Lokhorst (Eds.), *EFITA conference* (pp. 523–529). Wageningen, The Netherlands: Wageningen Acad Publ.

McCutchan, H., & Shackel, K. A. (1992). Stem water potential as a sensitive indicator of water stress in prune trees (*Prunus domestica* L. cv French). *Journal of the American Society Horticultural Science, 117*, 607–611.

Mirás-Avalos, J. M., Trigo-Córdoba, E., Bouzas-Cid, Y., & Orriols-Fernández, I. (2016). Irrigation effects on the performance of grapevine (*Vitis vinífera* L.) cv. 'Albariño' under the humid climate of Galicia. *OENO One, 50*(4), 183–194.

Montoro, A., Mañas, F., & López-Urrea, R. (2016). Transpiration and evaporation of grapevine, two components related to irrigation strategy. *Agricultural Water Management, 177*, 193–200.

Moral, F. J., Terrón, J. M., & Marques da Silva, J. R. (2010). Delineation of management zones using mobile measurements of soil apparent electrical conductivity and multivariate geostatistical techniques. *Soil and Tillage Research, 106*, 335–343.

Nendel, C. (2010). Grapevine bud break prediction for cool winter climates. *International Journal of Biometeorology, 54*, 231–241.

Netzer, Y., Yao, C., Shenker, M., Bradvo, B., & Schwartz, A. (2009). Water use and the development of seasonal crop coefficients for Superior Seedless grapevines trained to an open-gable trellis system. *Irrigation Science, 27*, 109–120.

Oyarzun, R. A., Stöckle, C. O., & Whiting, M. D. (2007). A simple approach to modeling radiation interception by fruit-tree orchards. *Agricultural and Forest Meteorology, 142*, 12–24.

Phogat, V., Skewes, M. A., McCarthy, M. G., Cox, J. W., Simunek, J., & Petrie, P. R. (2017). Evaluation of crop coefficients, water productivity, and water balance components for wine grapes irrigated at different deficit levels by a sub-surface drip. *Agricultural Water Management, 180*, 22–34.

Picón-Toro, J., González-Dugo, V., Uriarte, D., Mancha, L. A., & Testi, L. (2012). Effects of canopy size and water stress over the crop coefficient of a "Tempranillo" vineyard in south-western Spain. *Irrigation Science, 30*, 419–432.

Prats-Llinàs, M. T., Nieto, H., DeJong, T. M., Girona, J., & Marsal, J. (2020). Using forced regrowth to manipulate Chardonnay grapevine (*Vitis vinifera* L.) development to evaluate phenological stage responses to temperature. *Scientia Horticulturae, 262*, 109065.

Roby, G., Harbertson, J. F., Adams, D. A., & Matthews, M. A. (2004). Berry size and vine water deficits as factors in winegrape composition: anthocyanins and tannins. *Australian Journal of Grape and Wine Research, 10*, 100–107.

Santesteban, L. G., Miranda, C., & Royo, J. B. (2011). Regulated deficit irrigation effects on growth, yield, grape quality and individual anthocyanin composition in *Vitis vinifera* L. cv. 'Tempranillo.' *Agricultural Water Management, 98,* 1171–1179.

Scharwies, J. D. (2013) Water transport in grape berry and pre-harvest berry dehydration. School of Agriculture, Food and Wine. The University of Adelaide https://digital.library.adelaide.edu.au/dspace/bitstream/2440/82001/8/02whole.pdf.

Shackel, K., Ahmadi, H., Biasi, W., Buchner, R., Godhamer, D., Gurusinghe, S., Hasey, J., Kester, D., Krueger, B., Lampinen, B., McGourty, G., Micke, W., Mitcham, E., Olson, B., Pelletrau, K., Philips, H., Ramos, D., Schwankl, L., Sibebett, S., Snyder, R., Southwick, S., Stevenson, M., Thorpe, M., Weinbaum, S., & Yeager, J. (1997). Plant water status as an index of irrigation need in deciduous fruit trees. *HorTechnology, 7*, 23–29.

Stöckle, C. O., Donatelli, M., & Nelson, R. (2003). CropSyst, a cropping systems simulation model. *European Journal of Agronomy, 18*, 289–307.

Suay, R., Martinez, P. F., Roca, D., Martinez, M., Herrero, J. M., & Ramos, C. (2003). Measurement and estimation of transpiration of a soilless rose crop and application to irrigation management. *Acta Horticulturae, 614*(625), 630.

Sun, L., Gao, F., Anderson, M. C., Kustas, W. P., Alsina, M. M., Sanchez, L., Sams, B., McKee, L., Dulaney, W., White, W., Alfieri, J. G., Prueger, J. H., Melton, F., & Post, K. (2017). Daily mapping of 30 m LAI and NDVI for grape yield prediction in California vineyards. *Remote Sensing, 9*, 317.

Teixeira, A. Hd. eC., & Bassoi, L. H. (2009). Crop water productivity in semi-arid regions: From field to large scales. *Annals of Arid Zone, 48*(3), 1–13.

Towers, P. C., Strever, A., & Poblete-Echevarría, C. (2019). Comparison of vegetation indices for leaf area index estimation in vertical shoot positioned vine canopies with and without grenbiule hail-protection netting. *Remote Sensing, 11*, 1073.

Uribeetxebarria, A., Arnó, J., Escolà, A., & Martínez-Casasnovas, J. A. (2018). Apparent electrical conductivity and multivariate analysis of soil properties to assess soil constraints in orchards affected by previous parcelling. *Geoderma, 319*, 185–193.

Weiss, M., & Baret, F. (2016) *S2ToolBox level 2 products: LAI, FAPAR, FCOVER—Algorithm theoretical basis document*. Retrirved from http://step.esa.int/docs/extra/ATBD_S2ToolBox_L2B_V1.1.pdf.

Williams, L. E. (2017). Physiological tools to assess vine water status for use in vineyard irrigation management: review and update. *Acta Horticulturae, 1157,* 151–166.

Zalom, F. G., Goodell, P. B., Wilson, L. T., Barnett, W. W., & Bentley, W. J. (1983) Degree-days: The calculation and use of heat units in pest management. Cooperative Extension. Educational Agency of the University of California.

Zuñiga, M., Ortega-Farías, S., Fuentes, S., Riveros-Burgos, C., & Poblete-Echevarrría, C. (2018). Effects of three irrigation strategies on gas Exchange relationships, plant water status, yield components and water productivity on grafted Carménère grapevines. *Frontiers in Plant Science, 9*, 992.